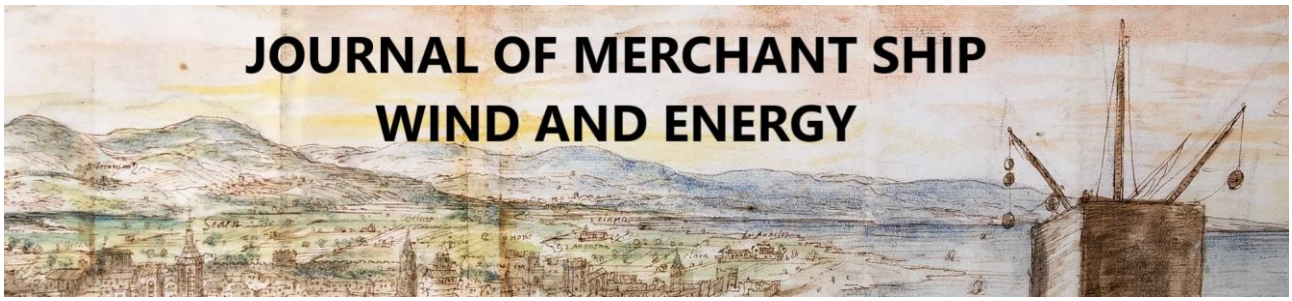

JMWE (https://www.jmwe.org) is an open and free peer-reviewed journal published under the CC BY-NC-SA 4.0 Creative Commons License. Image adapted from Anton van den Wyngaerde, 1653

Propeller-Sail vs. Flettner rotor Velocity Prediction Program results

Sergio E. Perez, Ph.D., Editor, jmwe.org, jmarwinden@gmail.com

Abstract

While full-size sails are the ideal for reducing emissions from sailing cargo ships, very large sails could limit access to ports or cargo. High-lift devices such as Flettner rotors and suction sails permit large lift forces from smaller sails, but require power input.

The Propeller-Sail is a novel, engine-powered high-lift device that is still under development. The concept consists of one or more propellers mounted on a ship wingsail, much like a multi-engine aircraft wing. The propellers, in this case mounted on the leading edge of the wingsail in so-called “tractor mode” have two beneficial effects:

- Increase the wingsail lift due to the high velocity of the propeller slipstream
- Create a thrust force in a direction opposite to the apparent wind, resulting in an effective decrease of drag on the wingsail that reduces ship downwind drift (leeway)

In this work, a tractor Propeller-Sail installed on a small cargo ship is simulated. A Velocity Prediction Program is used to determine the sailing performance of the rig, and compared to ships that are driven by normal marine propellers, Flettner rotors, and un-powered wingsails. We find that, at the same vessel velocities, the Propeller-Sail uses significantly less power than a normal engine-driven ship at True Wind Angles greater than about 55 degrees, and is also more economical to operate than an un-powered wing-sail working with partial engine assistance, at True Wind Angles greater than about 90 degrees. The Flettner rotor was found to use as little as 1/6 the power of the Propeller-Sail at the same speed, but it is noted that the Propeller-Sail can produce lift from the wind while using zero power.

Keywords: high-lift device, Propeller Sail, Propeller-Sail, Flettner rotor, suction sail, wing-sail, VPP

1. NOMENCLATURE

Advance ratio	$J = \frac{\mathrm{Vap}}{n\,D}\cos\theta$, where D is propeller diameter, n is rev/s, Vap is the apparent wind velocity entering propeller, and θ is the propeller angle of inclination into the flow
aspect ratio	A measure of wing slenderness, calculated by sail height^2 /wing area and height/diameter for a Flettner rotor.
chord	Wing-sail length from airfoil leading edge to trailing edge.
freestream velocity	Velocity upstream of a wing/propeller. In this case, the apparent wind speed.
slipstream velocity	Velocity behind the propeller, or the velocity experienced by the wing.

D	Drag force = $\frac{1}{2}\rho\, V^2 A\, C_d$	[1]
L	Lift force = $\frac{1}{2}\rho\, V^2 A\, C_l$	[2]
Tc	Thrust coefficient = $\frac{Thrust}{\frac{1}{2}\rho\, V^2 A}$	[3]

C_l	Aerodynamic lift coefficient based on freestream velocity
C_d	Aerodynamic drag coefficient based on freestream velocity
Tc	Propeller thrust coefficient based on freestream velocity
C_l "	Aerodynamic lift coefficient based on slipstream velocity
C_d"	Aerodynamic drag coefficient based on slipstream velocity
Tc"	Propeller thrust coefficient based on slipstream velocity
A	wing-sail area, wing height x mean chord
c	wing chord
T	Thrust
Vap	Apparent wind speed
Re	Reynolds number, Re $= \frac{Vap\, c\, \rho}{\mu}$
ρ	Fluid density
μ	Fluid dynamic viscosity

NACA	National Advisory Committee on Aeronautics
VPP	Velocity Prediction Program

2. INTRODUCTION

The Propeller-Sail is a new concept, and is still under development (please see Figure 1). The idea consists of mounting engine-powered propellers on ship wing-sails in order to increase lift and decrease sail size, with the goal of reducing fuel use.

Using very large sails is the ideal from an economics and environmental point of view, but can be impractical. In a report to the U.S. Maritime Administration (Woodward et al.,1975), the authors found that mast heights in excess of 90 m would be required for a 50,000 CDWT sailing cargo vessel, for similar performance to large sailing ships of the past. High-lift devices such as Flettner rotors, suction sails and Propeller-Sails can generate greater lift forces than conventional sails, permitting the use of smaller sails. Of course, these devices require power to generate an enhanced driving force, and the power used must be significantly less than that required by the ship's engines to drive the ship.

Preliminary 2-Dimensional (representing motion and forces only along the axis of a ship's length and the axis of a ship's mast) CFD (Computational Fluid Dynamics) studies of the Propeller-Sail were performed in Perez (2023a). It was found that: propellers mounted on wing-sails increase lift and drag, flaps could increase the effect of the propellers, and that a pusher configuration created about the same thrust and less drag than mounting the propellers in the more conventional tractor mode.

Figure 1. Propeller-Sail remote-control model

3-Dimensional CFD (Computational Fluid Dynamics) simulations were performed on a NACA0020 unflapped wing with 2 propellers in pusher mode in Perez and Ribarov (2023), at angles of attack as great as 60 degrees. A trend was observed showing two distinct propeller power regimes: one at low propeller rotation speeds, which exhibited lift force increasing rapidly with increased propeller rotation speed, and another at higher rotation rates, in which lift increased at a slower rate. The authors postulated that in the first regime, increased propeller rotational speeds augmented lift by increasing the flow speed over the wing and by reducing separation due to propeller suction. In the second regime, where flow was more fully attached to the wing, lift only increased due to greater flow velocity. In addition, basic remote-control model tests demonstrated that a 1-m model ship (Figure 1) moved well using powered and un-powered Propeller-Sails, showing that the concept is practicable.

In the current work, experimental results with powered wings at high angles of attack are used to predict lift, drag and power consumption of a Propeller-Sail in tractor mode. Specifically, Kuhn and Draper (1954a,b) conducted wind tunnel experiments of tractor-propeller-powered, high angle of attack, flapped and unflapped wings for VTOL/STOL (Vertical Take-Off and Landing/Short Take-off and Landing) aircraft. The results of these experiments are directly applicable to the analysis of a Propeller-Sail in tractor mode.

3. THE PROPELLER-SAIL SIMULATION

In the current work, a scaled-up version of a rig tested in a wind tunnel by Kuhn and Draper (1954a) is used to predict the performance of a Propeller-Sail. The propellers in the rig are quite large in relation to the wing, presumably to permit a propeller airplane to take off vertically by vectoring the propeller slipstream towards the ground using articulated flaps.

The Propeller-Sail rig consists of a NACA 0015 wing section, with a flap measuring 30% of the wing chord, set to a 30-degree flap deflection angle, as shown in Figure 2. The wing is set to an angle of attack of 16 degrees for all of the simulations, which restricts the simulations to True Wind Angles of about 125 degrees and less. Only a wind speed of 10 m/s is used in this study.

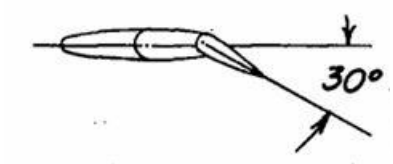

Figure 2, from Kuhn. NACA 0015 wing section used in the current work.

Figure 3 shows the entire rig, which is half of an entire aircraft wing, referred to as a “semi-span”. Two propellers are shown, but only the one-propeller, inboard engine results from Kuhn (1954a) are used, as the power to turn both propellers was excessive. The inboard engine propeller turns counter-clockwise

(when viewed from aft). The semi-span was attached to the wind tunnel ceiling, in a similar way as a wing-sail might be connected to the deck of a ship.

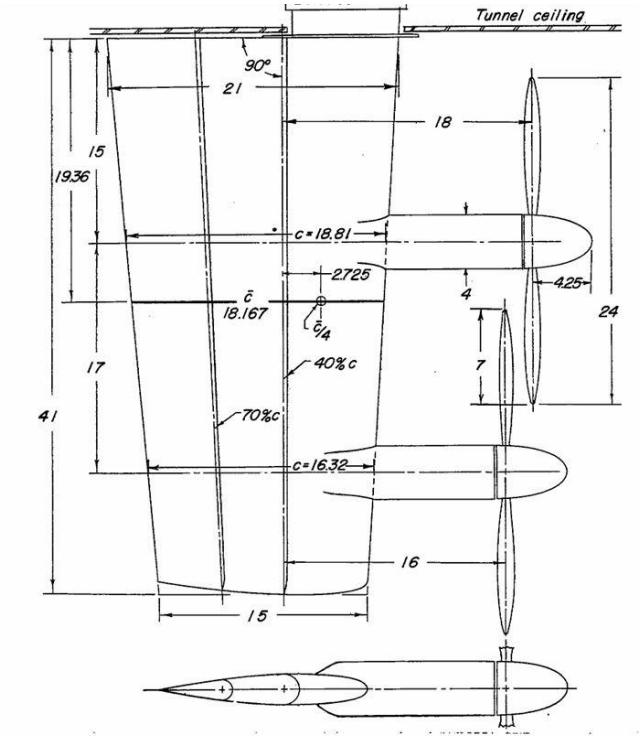

Figure 3. Half-span wing and engines. The current work uses Kuhn (1954a) wind tunnel data with inboard engine only, with the outboard engine and nacelle removed. Note the large size of the propeller relative to the wingspan; normal propeller aircraft would use less than half the size shown. Dimensions are in inches.

The characteristics of the Propeller-Sail analyzed in this work are presented in Table 1, below. The design is a scaled-up version of Kuhn's (1954a) experimental rig.

Wing-sail	**Height**: 13 m, **Area**: 75 m^2, **Base chord**: 5.74 m, **Tip chord**: 4.8 m, **Aspect Ratio** (geometric):4.55, **Aspect Ratio** (effective): 9.11 (Olsen, 2016) **Wing angle of attack**: 16 degrees, **Flap deflection angle**: 30 degrees, **Flap size**: 30% of chord, **Wing mounting**: on horizontal deck
Propeller	**Diameter**:7.66 m, **Blades**: 3, with Clark Y shape, **Blade angle**: 20 degree at 0.75 Radius, at low thrust modes used in this work, **Efficiency**: max of 60%; **Rotational speed**: 2- 4 rev/s with 10 m/s wind speed
Rig performance	**Powered Lift coefficient**: 2.2, **Drag coefficient**: 0.16, **Power used (in 10 m/s wind)**: 32-80 kW, depending on ship angle to relative wind, **Cl and Cd with un-powered propeller**: 1.7, 0.4
Reynolds number	**Kuhn (1954a) Model in wind tunnel**: $= 8\ x\ 10^5$, **Full scale Propeller-Sail**: 4-7 $x\ 10^6$

Table 1. Rig characteristics.

3.1 Reynolds number dependence

The experimental Reynolds number used in Kuhn (1954a) was $8\ x\ 10^5$, based on the propeller slipstream velocity. The Propeller-Sail Reynolds number is based on an estimated propeller slipstream velocity ranging between 12.4 m/s and 18.6 m/s (calculated using equations given in Kuhn (1954a)). Propeller-Sail Reynolds numbers were then between 5 and 8 times greater than Kuhn's experiments.

The effect of this larger Reynolds number on Propeller-Sail Cl and Cd values is difficult to estimate due to a paucity of experimental information on flapped wings operating at stall, with propellers attached. Based on early results from Jacobs (1939), one would expect maximum lift coefficients to increase with increasing Reynolds numbers, and drag coefficients to decrease at the same lift coefficient. For a flapped NACA 0012 airfoil, the increase in the max lift coefficient (at incipient stall) due to an increase in Reynolds number from $8\ x\ 10^5$ to $6\ x\ 10^6$ would be at least 13%. For an unflapped, almost stalled NACA 0015 wing, the drag coefficient would decrease by about 15%. Based on these results, it may be inferred that the Propeller-Sail rig in the current work would probably produce higher lift and lower drag than predicted here.

3.2 Equations used

Normally, lift, drag and thrust coefficients Cl, Cd and Tc are non-dimensionalized using the freestream velocity (apparent wind speed in our case) using equations 1-3.

Kuhn's (1954a) results give lift (Cl"), drag (Cd") and propeller thrust (Tc") coefficients based on the propeller slipstream velocity (the air speed behind the propeller), for a wide range of articulated flap positions and wing angles of attack. Conversions can be made between the two using the equations listed below.

Note that total lift and drag forces (L and D) are the sum of the wing forces and any propeller thrust components. The propeller thrust reduces total wing drag, and increases wing lift when the propeller is angled upwards (as occurs here at 16 degree wing angle of attack), as shown in Figure 4, below:

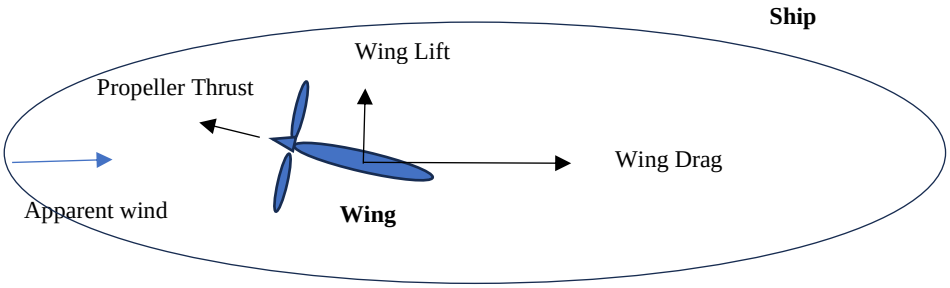

Figure 4. The Propeller-Sail seen from above, installed on a ship. Note that the propeller thrust augments lift and tends to decrease drag of wing/propeller unit.

In the current work, equations for maximum (at stall) Cl" and Cd" were obtained from Kuhn's (1954a,b) data, as a function of thrust coefficient Ct". Equations were fit for the configuration from Kuhn which gave the highest lift coefficient, namely the NACA 0015 wing at 16 degrees angle of attack (at stall point), with flap set to 30 degree deflection.

From Kuhn's (1954a) data, curve fits in equations 4-5 were calculated:

$$Cl" = -1.5\,Tc"^2 + 0.05\,Tc" + 1.6 \qquad [4]$$

$$Cd" = -(0.63333\,Tc"^2 + 0.97667\,Tc" - 0.37) \qquad [5]$$

Equation 6-9 are used to calculate the full-scale propeller thrust, lift and drag, given the apparent wind velocity Vap and Tc":

$$Thrust\ T = \frac{\rho\ \Pi\ Vap^2\ Dp^2}{8\ \{\frac{1}{Tc"} - 1\}} \qquad [6]$$

$$Lift\ L = Cl"\ (\ q\ +\ \frac{4\ T}{\Pi\ Dp^2}\ )\ x\ Awing \qquad [7]$$

$$Drag\ D = Cd"\ (\ q\ +\ \frac{4\ T}{\Pi\ Dp^2}\ )\ x\ Awing \qquad [8]$$

Where Awing is the wing area, ρ is the air density, Vap is the apparent wind speed, Dp is the propeller diameter, Tc" is the thrust coefficient from Kuhn, Cl" and Cd" are Kuhn wind tunnel lift and drag coefficients, and q is the dynamic pressure based on Vap:

$$q = \frac{1}{2}\ \rho\ Vap^2 \qquad [9]$$

The expression $\frac{4\ T}{\Pi\ Dp^2}$ in equations 7 and 8 represent the dynamic pressure due to the propeller slipstream.

It is interesting to see the effect of increasing propeller power on the drag coefficient. Figures 5a and 5b show the drag coefficients Cd and Cd", as well as lift coefficients Cl and Cl". As the propeller power is increased, the drag coefficient Cd drops, and eventually reaches a value of zero at a Tc" value of about 0.7. However, the power required to turn the propellers at this Tc" would be prohibitively large.

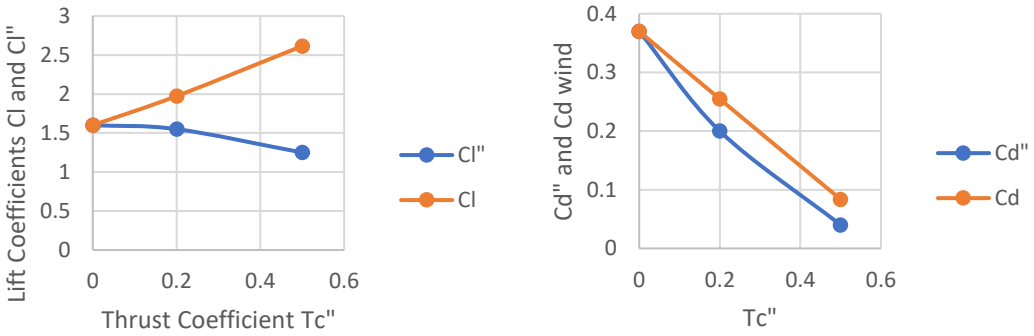

Figure 5a (at left) and 5b. Cl and Cl", and Cd and Cd" as a function of Tc". Note that the drag coefficient Tc" becomes zero at a thrust coefficient of about 0.7, due to the thrust of the engine.

Propeller power is calculated by taking the product of thrust and apparent wind velocity Vap, and dividing by 0.6, which is the maximum efficiency of the propeller used in Kuhn (1954a,b), at an advance ratio of 0.72. The apparent wind velocity is multiplied by the cosine of 16 degrees to account for the inclination of the propeller.

The propeller's proximity to the wing in Kuhn(1954b) and tunnel wall have considerable effect on the propeller efficiency: operating by itself (with neither the wing nor tunnel wall nearby), the propeller efficiency was 0.77. It is noted that with 10 m/s winds, the apparent wind speeds would vary between 10 and 20 m/s, requiring relatively low propeller rotational speeds between 1.8 and 3.6 rev/s at the high efficiency advance ratio of 0.72.

Equations 4-9 are used as input to the velocity prediction program VPP, which then calculates vessel speed and track. The thrust coefficient Tc" and wind speed are required inputs for a VPP run.

3.3 The Velocity Prediction Program (VPP)

OpenVPP (Perez, 2023c) is an open-source product that explicitly solves the sailing vessel equations of motion. The program uses a 4th order Runge-Kutta scheme, and provides sailing vessel velocities as a

function of True Wind Angle and wind speed. The vessel modeled is a 36 m “Series-60” hull, assumed fully loaded, mounted with 75 m^2 of sail area.

There are two general techniques for solving the equations which result from analyzing the forces on a sailing vessel. The most common method is by setting the sum of forces to zero, and solving the algebraic equations simultaneously, or *implicitly*. This is sometimes referred to as an *equilibrium* method. The second technique, used in OpenVPP, involves allowing the vessel to begin at some initial velocity and direction, and suddenly applying a wind speed, from which forces on the vessel can be determined and hence its acceleration is known. The vessel is then allowed to accelerate through a small period of time or *time steps*, after which the vessel has a new speed and direction. After many repeated time steps (marching forward in time), the vessel eventually reaches a speed and heading that no longer change. This type of solution is known as, *explicit,* or *dynamic*. The advantage of the explicit scheme is that the solution method is somewhat easier. Equations do not need to be solved simultaneously. Instead, the known velocity and orientation at time = 0 are used to extrapolate to future steady values. In addition, the technique may be used to solve for unsteady parameters such as acceleration, rate of turn or response to wave action (OpenVPP does not do this in its current form).

OpenVPP assumes that ship roll (heel) due to wind force is less than about 10 degrees, and therefore has little effect on the performance of a large sailing ship. This is a reasonable assumption since, for similar hulls, heeling moment varies by the 3rd power of the ship length, while righting moment varies by the 4th power (Skene, 1973). Vessels of this magnitude are then likely to be very resistant to roll.

OpenVPP also assumes that the vessel is balanced in yaw, so the effect of rudders is not considered. This is appropriate for the purpose of evaluation and comparison of designs as part of a first loop of a design-spiral.

3.4 Simulations

The Propeller-Sail was simulated in 10 m/s (20 knots) winds, using a lift coefficient Cl of 2.2. This is a rather low lift coefficient for a high lift device, but larger than the same flapped airfoil without the engines and nacelles, with a lift coefficient of about 1.7. Using the powered Propeller-Sail instead of the un-powered wing would result in a 30% reduction in wing area, for the same lift force and wind speed.

The relatively low lift coefficient is used because of the small slope exhibited in Figure 6, for the power required as a function of Propeller-Sail lift coefficient Cl, at a True Wind Angle of 98 degrees and 10 m/s winds. Increasing the lift coefficient by 10% from 2 to 2.4 would require a power increase of 63%.

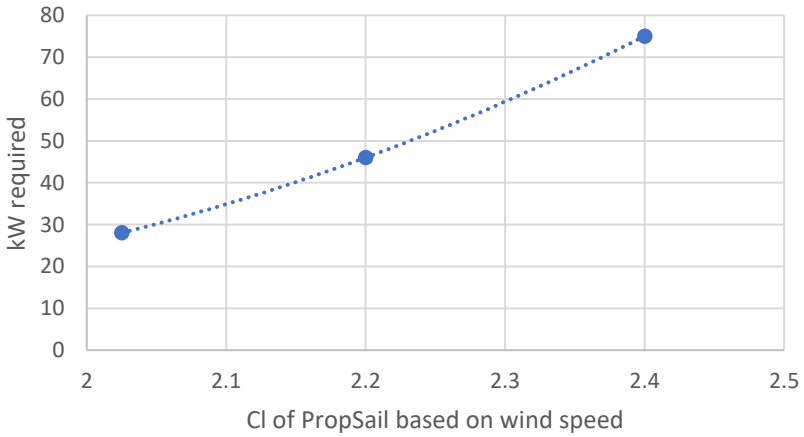

Figure 6. Propeller-Sail power as a function of lift coefficient Cl, at vessel True Wind Angle of 98 degrees and 10 m/s winds.

We distinguish between several operational modes: *propeller-sail*: the powered, wing-mounted propeller used in conjunction with the wind, *pure sailing mode*: the Propeller-Sail used without the air propeller activated and the ship's engine off, *engine-assist mode*: the unpowered wing-sail used in conjunction with the ship's engine/propeller, *normal cruising mode*: the ship powered only by the ship's engine, *Flettner mode*: a Flettner rotor used to drive the ship in wind.

In order to compare the Propeller-Sail to the engine-assist mode, an efficiency of 0.8 was assumed for a ship's normal propeller, while the Propeller-Sail propeller efficiency was taken as 0.6 (Draper and Kuhn, 1954b). A higher efficiency was assigned for the marine propeller because of the well-known efficiency boost from operating behind hulls (Zubaly, 1996). In addition, as stated earlier, propellers acting on wings have reduced efficiency.

4. COMPARING THE PROPELLER-SAIL WITH OTHER PROPULSION ALTERNATIVES USING A VELOCITY PREDICTION PROGRAM (VPP)

4.1 Propeller-Sail vs. Normal Cruising Mode:

In this analysis the powered Propeller-Sail is compared with the ship's normal powered cruising mode, assuming the ship moves at the same speed with both configurations.

The power required to move the vessel in cruising mode was calculated in the VPP by adding 20% to the towing tank results to account for the increase in drag caused by the ship's propeller (Zubaly, 1996), and then taking the product of drag force and velocity, divided by 0.8 to account for the ship propeller's efficiency. When using the powered Propeller-Sail, it is assumed that the marine propellers (that is, propellers in the water) are feathered or folded, and have no effect on the resistance of the hull.

4.2 Flettner rotor vs. Propeller-Sail

Ideally, when comparing the Propeller-Sail with Flettner rotors, the two devices should have the same aspect ratio (so neither has an induced drag advantage), the same volume (to account for vessel space lost) and the same height (to account for air draft limits). But accounting for all three is impossible, and it was decided that volume and heights of Flettner and Propeller Sail should be the same. The volume of the Flettner rotor was calculated by multiplying the area of the circular rotor face by the height of the cylinder. The volume of the Propeller-Sail was calculated by the product of the NACA 0015 profile face and the height of the wing.

The performance of the Propeller-Sail was compared with that of a Flettner rotor of 15 m height and 2.08 m diameter. The Flettner spin ratio was determined by assuming the same lift force as the Propeller-Sail (which uses a lift coefficient Cl of 2.2 for all VPP results), in conjunction with polynomial curve fits for spin ratio (apparent wind speed/Flettner tangential velocity) as a function of lift coefficient derived from experimental results in Kwon et al. (2022), for a rotor with an aspect ratio of 6. Also derived from the same paper was an equation for the power coefficient cp, as a function of the rotor tangential velocity and rotor area, permitting calculation of aerodynamic power required to spin the rotor. The Flettner geometric aspect ratio of 6 gives it an induced drag advantage over the Propeller Sail, which has a geometric aspect ratio of 4.55. Both configurations had about the same vessel speed when the same lift force was applied.

It should be mentioned that making the Flettner and Propeller-Sail have equal volumes and heights results in the Flettner requiring lift coefficients of about 6 in order to generate the same lift force as a Propeller-Sail at Cl of 2.2, since the chord of the Propeller-Sail wing is about 5 m, and the diameter of the Flettner is 2 m. Both of these are used to calculate the area A, which is used to calculate lift in the equation below:

$$\text{Lift force} = \frac{1}{2}\rho\, V^2 A\, C_l \qquad [10]$$

This would not be a drawback for the Flettner rotor unless lift coefficient values greater than 10 are required, which is usually the limit of use of the Flettner rotor. The Propeller-Sail lift coefficients which would push the Flettner into such high Cl values are too high to be efficient, as tested in the current work.

The effect of bearing friction on the power required to spin the rotor is not available in the open literature, and is estimated here using marketing data from bearing and Flettner manufacturers. The mass of an existing Flettner rotor measuring 18 m high x 4 m diameter is 27 tons, and is scaled to the volume of the simulated rotor (50.97 m^3) to determine the mass of the simulated Flettner. Once the weight of the rotor is known, the frictional rotational force is calculated using the frictional coefficient for the bearings of 0.0015 (American Roller Bearings, 2024). This permits the elementary calculation of torque and power required to turn the Flettner rotors.

Both the Propeller-Sail and Flettner rotor modes were assumed to operate on a ship with folding or feathered marine propellers that have no effect on the resistance of the hull.

4.3 Propeller-Sail vs. Engine-Assist

In this analysis the un-powered Propeller-Sail (Cl = 1.7, Cd = 0.4) with propellers stationary is used concurrently with the ship's normal engine/propeller, and compared with the powered Propeller-Sail at the same vessel speed. In other words, is it better to simply use an unpowered Propeller-Sail to aid the normal ship's propulsion? (the exact position of the stationary propellers is unspecified in Kuhn (1954a,b).

In the VPP, the thrust from the ship's engine was accounted for as a reduction in the total drag of the vessel. The engine power used was calculated by taking the product of the reduction in drag force and the resulting vessel speed (as determined by the VPP), modified by the thrust deduction factor and propeller efficiency, as described above in section 4.1. The amount of engine thrust applied was specified using the percent reduction in ship drag; for example, *30% engine-assist* reduces the ship's drag by 30%.

By a trial-and-error process, it was found that using 30% engine assist in 10 m/s winds results in a vessel speed approximately equal to that of the Propeller-Sail mode.

4.4 Pure sailing mode

Figure 10 shows that using one wing in pure sailing mode results in as much as 2.2 knots (25%) lower speed than the Propeller Sail, at 10 m/s wind speed.

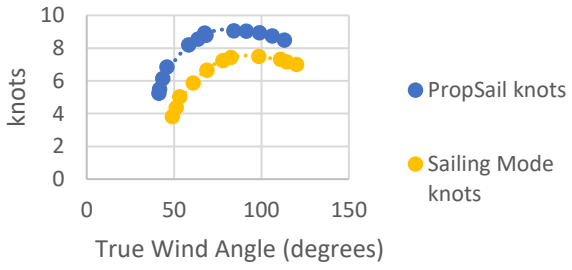

Figure 10. The Propeller-Sail compared with un-powered Propeller-Sail (pure sailing mode) in 10 m/s winds.

5. RESULTS AND CONCLUSIONS

Figure 11, below, displays the VPP-determined power required for the four analyzed operational modes, in 10 m/s winds, on a 36 m cargo vessel. All of the modes operated at approximately the same vessel speeds at each wind angle. The four operational modes are summarized:

- Propeller-Sail at a lift coefficient of 2.2
- the Flettner rotor, operating at the same lift force as the Propeller-Sail
- normal vessel cruising mode with ship's engines activated
- engine assist mode (un-powered Propeller-Sail acting as a wingsail, aided by the ship's engine at 30% level. This setting produced the same vessel speed as the Propeller-Sail)

The plots in Figure 11 show the power consumed in each mode, at three True Wind Angles: 60, 100 and 125 degrees. The figure clearly shows that the Flettner rotor uses considerably less fuel than the other modes, at all wind angles.

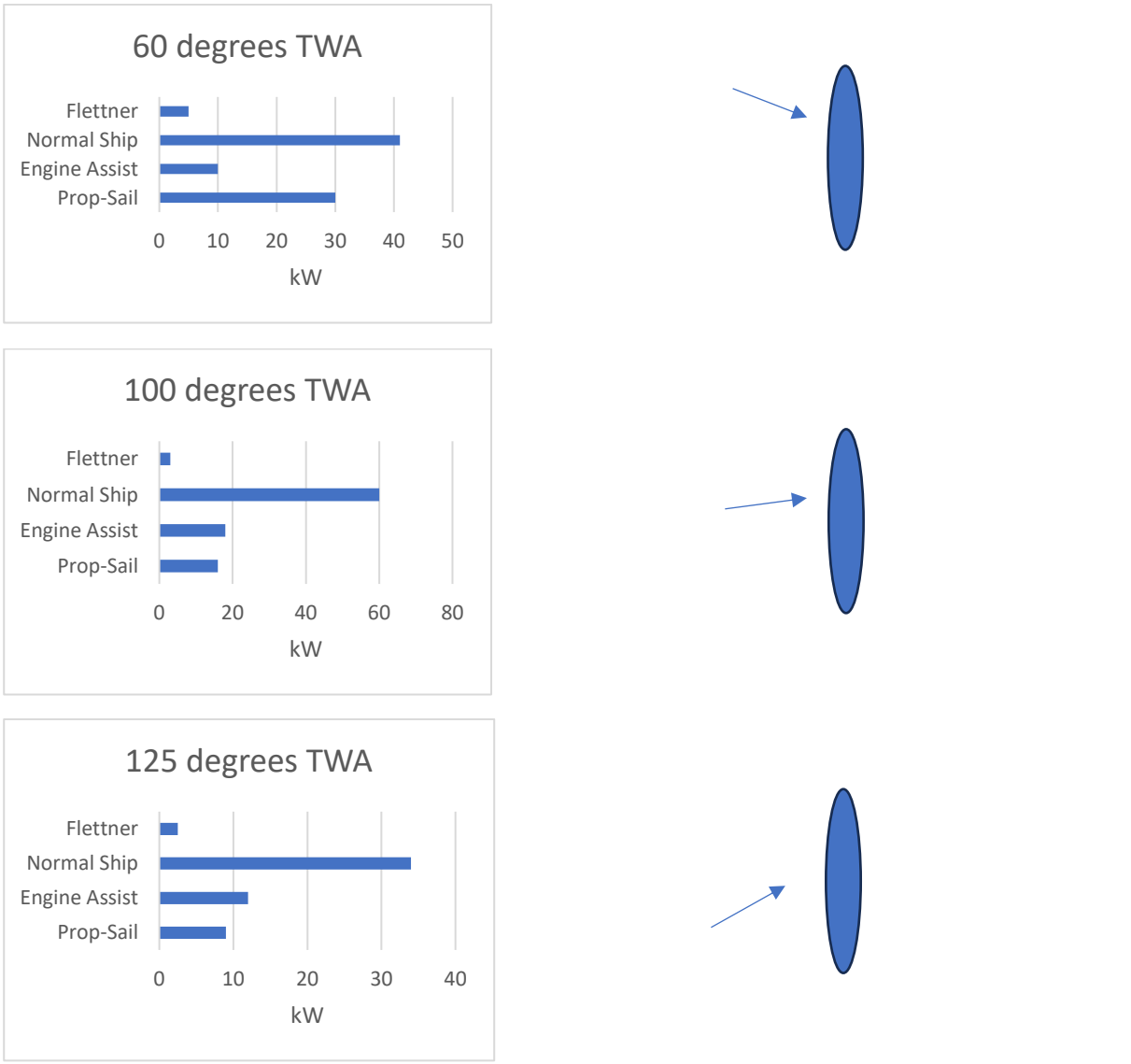

Figure 11. The power required (kW) results for the 4 modes investigated, at differing True Wind Angles. Vessels are at equal speeds on each plot, ranging from 5 – 9 knots. The ships are moving upwards.

Ignoring the Flettner for the moment, the engine-assist and Propeller-Sail modes outperform the normal ship at all wind angles, especially the larger ones.

Figure 11 points to a strategy for effective use of the Propeller-Sail: at low True Wind Angles, the engine assist mode (un-powered Propeller-Sail acting as a wing-sail) is best. At wind angles around 100 degrees and beyond, the Propeller-Sail should be energized. This will provide significant reductions in power use, as low as 1/5 the power, as compared to the normally operating ship.

Despite the superiority of the Flettner rotor, the Propeller-Sail has some features that the Flettner lacks: it can provide thrust from the wind with zero power use, and it can be feathered into the wind without using power in the event of overly strong winds. The Flettner must be motor-driven to achieve low drag.

It is also possible that a Propeller-Sail could serve as a thruster for maneuvering, or perhaps entirely replace a ship's normal propeller for sailing vessels operating at lower speeds. The author noted the simplicity of constructing a Propeller-Sail model that is powered solely by the Propeller-Sail rig, without the need to make and maintain a through-the-hull shaft.

It is safe to say that at least, the idea merits further research.

REFERENCES

American Roller Bearings (2024). https://www.amroll.com/friction-frequency-factors.html

Kuhn, R. and Draper, J. (1954a), An investigation of a wing-propeller configuration employing large chord flaps and large diameter propellers for low-speed flight and vertical take-off, NACA Technical Note 3307, 1954, Langley Aeronautical Laboratory

Draper, J., Kuhn, R. (1954b) An investigation of the aerodynamic characteristics of a model wing-propeller combination and of the wing and propeller separately at angles of attack up to 90 degrees, NACA Technical Note 3304, Langley Aeronautical Laboratory.

Jacobs, E., and Sherman, A. (1939), Airfoil section characteristics as affected by variations of the Reynolds number, NACA Report 586, 1939

Kwon, C.S., Yeon, S.M., Kim, Y.C., Kim, Y.G., Kim, Y.H., Kang, H.J. (2022). Parametric study for a Flettner rotor in standalone condition using CFD, International Journal of Naval Architecture and Ocean Engineering 14 (2022) 10049 https://doi.org/10.1016/j.ijnaoe.2022.100493

Norsepower Website, (2024). https://www.norsepower.com/technical-info/

Olssen, L., Eliasson, R., Orych, M. (2016), Principles of Yacht Design, 4th edition, McGraw Hill Publishers.

Perez S. (2023a). Preliminary Analysis of a new high lift device for sailing cargo ships using distributed wing-mounted propellers, Journal of Merchant Ship Wind Energy, February 2023, https://www.jmwe.org

Perez S. and Ribarov L. (2023b). A second look at the Propeller Sail high lift device for sailing cargo ships, using distributed, wing-mounted propellers, S. Perez and L. Ribarov, Journal of Merchant Ship Wind Energy, November 2023, https://www.jmwe.org

Perez, S. (2023c). OpenVPP: An Open-Source Dynamic Velocity Prediction Program for sailing cargo vessels, Journal of Merchant Ship Wind and Energy, January 2023, https://www.jmwe.org

Skene, N. (1973), Skene's Elements of Yacht Design; Francis Kinney, Dodd, Mead and Company

Todd, F.H. (1963). Series 60 methodical experiments with models of single-screw merchant ships, David Taylor Model Basic Report 1712

Wagner, B. (1967). Wind tunnel tests for a six-masted sailing vessel by Prölss: Translation of B. Wagner's Windkanalversuche für einen sechsmastigen Segler nach Prölss", L.A. Ribarov, Journal of Merchant Ship Wind Energy, September 2022, https://www.jmwe.org

Wagner,B. (1968). Translation of Wagner's Angled towing tests for a sailing vessel hull with and without bar keel and for the "Mariner" (Schrägschleppversuche für einen Seglerrumpf mit und ohne Balkenkiel und für den "Mariner"); L.A. Ribarov, September 2022, Journal of Merchant Ship Wind Energy www.jmwe.org

Woodward, J., Beck, R., Scher, B., and Cary, C. (1975). Feasibility of sailing ships for the American merchant marine; Report #168, Feb 1975, University of Michigan Department of Naval Architecture and Marine Engineering, report to the U.S. Maritime Administration

Zubaly,R. (1996). Applied Naval Architecture, Cornell Maritime Press, 1996